Robust LQG Controller Design by LMI Approach of a Doubly-Fed Induction Generator for Aero-Generator

Article · December 2022

DOI: 10.18280/jesa.550613

CITATION
1

READS
129

3 authors:

Mohand Said Larabi
Université 20 août 1955-Skikda
6 PUBLICATIONS **5** CITATIONS
SEE PROFILE

Said Yahmedi
Badji Mokhtar - Annaba University
17 PUBLICATIONS **36** CITATIONS
SEE PROFILE

Zennir Youcef
Université 20 août 1955-Skikda
110 PUBLICATIONS **393** CITATIONS
SEE PROFILE

IIETA International Information and Engineering Technology Association
Advancing the World of Information and Engineering

Journal Européen des Systèmes Automatisés
Vol. 55, No. 6, December, 2022, pp. 803-816
Journal homepage: http://iieta.org/journals/jesa

Robust LQG Controller Design by LMI Approach of a Doubly-Fed Induction Generator for Aero-Generator

Mohand Said Larabi[1,2*], Said Yahmedi[2], Youcef Zennir[1]

[1] Automatic Laboratory of Skikda, Université 20 Août 1955 Skikda, Skikda 21000, Algeria
[2] Laboratory of Mathematical Modeling and Numerical Simulation, Badji Mokhtar University, Annaba 23000, Algeria

Corresponding Author Email: y.zennir@univ-skikda.dz

https://doi.org/10.18280/jesa.550613

Received: 27 October 2022
Accepted: 16 November 2022

Keywords:
aero-generator, Linear Quadratic Gaussian (LQG), Linear Matrix Inequality (LMI), Doubly Fed Induction Generator (DFIG), singular values, robustness conditions, Lyapunov stability

ABSTRACT

This article presents a design method to improve the robustness in stability and performance of an LQG controller by the LMI approach applied to a multivariable system subject to parametric uncertainties, where its variations are known to have a direct impact on the degradation of the robustness margins of a classical LQG controller. The main of this work is to synthesize a robust Linear Quadratic Gaussian (LQG) controller reformulated by the Linear Matrix Inequality (LMI) approach and to apply it on an ill-conditioned system. Our choice fell on a doubly fed induction generator (DFIG) of the aero-generator to produce electrical energy, whose physical parameters are uncertain due to several factors: winding heating, magnetic saturation..., this makes it difficult to maintain the voltage at 220V and the frequency at 50Hz. First, the mathematical model of DFIG is written in a d-q reference frame. The singular values of the uncertainties are quantified and multiplied at the system output, and then the robustness conditions are determined. Secondly, the robust control law by the LQG synthesis based on the solution of the convex optimization problem under LMI Eigenvalue problem is elaborated and detailed. The simulation results of the stability and performance robustness of the LQG controller by the LMI approach with nominal and disturbed model of the DFIG are presented and discussed on the method efficiency.

1. INTRODUCTION

Wind energy is one of the various renewable energy sources used to produce clean electric energy without any pollution and which does not require any fuel (100% natural). Thus, in the winter, the electrical energy yield will be higher through wind power which covers the significant demand for energy consumption, for this reason the aero-generators are used to convert the wind's kinetic energy into electrical power [1]. The aero-generator is mainly equipped with a machine containing a doubly-fed induction generator (DFIG) because of its ease of construction and simplicity maintenance, reliability and minimal cost [2]. Nevertheless, it is difficult to maintain the voltage and frequency produced by the DFIG at the requested values (voltage equal to 220V and frequency equal to 50Hz), Due to the influence of disturbances which affect the good functioning of the generator, come primarily from the variations of the wind intensity at the blades level of wind turbine and the electrical energy consumption via the electrical network directly connected to DFIG [1, 2], see Figure 1.

In addition, control of the DFIG is quite difficult because of the coupling existing between the flux and the electromagnetic torque [3], which implies a nonlinear model, its linearization around the operating point leads to an approximate model. Thus, its parameters, resistances and cyclic inductances of the rotor and stator windings are variable due to the physical phenomena: Heating, magnetic saturation [3, 4], so that the behavior of the DFIG changes continually and causes a gap between its real and approximate model, these model uncertainties degrade the performances of the applied control and cause the operating instability of the DFIG. To overcome this problem, we propose to synthesize a robust controller which ensures stability and performances robustness conditions for the nominal and perturbed (uncertainty plant) operating modes. In this paper, we are interested the development of a robust control law by the LQG (Linear Quadratic Gaussian) synthesis, which is a combination of two parts [5, 6]: LQ (Linear Quadratic) state feedback control and Kalman Estimator, the resolution of this LQG stochastic control problem is known as the separation theorem [6-8] based on the minimization of a quadratic criterion.

This robust control method improves the performance of doubly-fed induction generators in terms of set-point tracking, parametric variations and sensitivity to disturbances [9]. However, the Kalman Estimator installed in the LQG controller weakens the good robustness properties of the LQ control by state feedback, an infinite gain margin, and a 60deg phase margin [10, 11]. To improve these properties of robustness [12-14], have demonstrated a new design based on LQG, LTR (Loop Transfer Recovery), which allows recovering the robustness properties of the LQ control by state feedback. The classic LQG regulator has proven its effectiveness in many control problems of linear systems with good robustness margins, however, when the systems are affected by parametric uncertainties, the classic LQG regulator becomes insufficient and loses its robustness.

To fix this problem, Our objective is to reformulate the classical LQG control problem by the LMI approach (Linear

Matrix Inequalities) based on the Lyapunov function to guarantee the asymptotic stability of the LQ control set and the estimator while keeping their good stability margins and to maintain the desired good performance in the presence of parametric uncertainties, which reinforces the LQG controller to ensure the conditions of robustness on the stability and the desired performance in closed loop. Therefore, it is proposed to introduce the method of Lyapunov to solve separately the two parts, Problem LQ and the Estimator, in LMI form, in order to ensure internal stability of the control loop and to satisfy the desired performances. The interest of the LMIs is that they can be solved by convex programming under the eigenvalue problem (LMI-EVP) by making a change of variables [15-17]. Its resolution is developed by an algorithm known as the point-interior method [16, 18], which gives two advantages to the convex optimization problem [19]:

The computing time to find a solution is reasonable. There is no local minimum of the cost function to optimize the result obtained corresponds to a single global minimum. Finally, the gain matrices of the Kalman estimator and the state feedback control are constructed from the solutions found.

This design technique of the LQG Robust controller by the LMI approach, applied to the uncertain DFIG model, shown in the simulation part a good trajectory tracking, as well as the maintaining of the output voltage at the set value of 220V and the frequency at 50Hz, despite the uncertainties of the DFIG model with the full guarantee of robustness conditions.

This paper is organized as follows:

Section 2 presents the (DFIG) doubly-fed induction generator description of the aero-generator, modeled by the Park's transformation and given in the state space. Section 3 presents the concepts of robustness conditions. Section 4 presents the robust LQG control synthesis method using LMI approach. Section 5 presents the simulation results of our application, which are presented in the frequency-domain and in the time-domain. Finally, the last section will be devoted to the conclusion.

2. GENERAL PLANT DESCRIPTION

The following figure shows the overall diagram of the process to be controlled, the aero-generator:

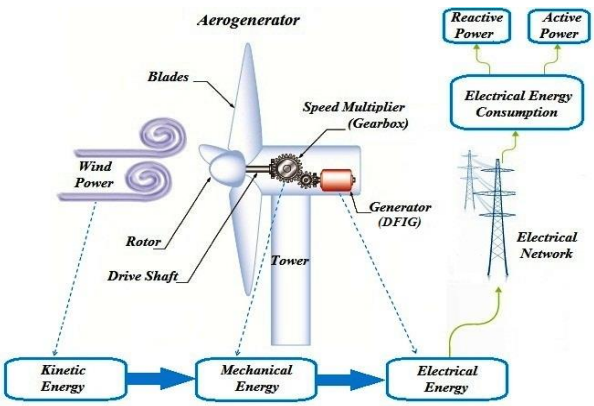

Figure 1. Aero-generator system

The aero-generator process uses two levels of energy conversion, the first is the conversion of kinetic energy from the wind into mechanical energy via the turbine (together, turbine rotor which is composed of blades and speed multiplier (Gearbox) mounted on the shaft [1]). The second transforms mechanical energy into electrical energy through a generator "DFIG" based on doubly-fed asynchronous machine where its stator is connected directly to the electrical network, as well as its rotor by means of a static converter to be able to send the commands of the robust controller supplied by the algorithm of LQG synthesis. And to control stator power (the output of the DFIG) to the same requirements of the electrical network power, with the following references: voltage and frequency respectively equal to 220Volts and 50Hz, whatever are the perturbations affecting the aero-generator; The variations of the wind speed and the electrical energy consumption under the shape of an active or reactive power. For more details on the modeling of Aero-generator see References [20-22].

The electrical equations of the doubly-fed induction generator (DFIG) are modeled by the Park transformation uses d-q reference frame on the stator and the rotor of DFIG, for more details see [23-25].

The dynamics of the process to be controlled is described by the following differential equations [9, 26-28]:

The components of the stator voltage vector are given by following equations [9, 26, 27]:

$$V_{ds} = R_s I_{ds} + \frac{d\Phi_{ds}}{dt} - \omega_s \Phi_{\mathrm{qs}} \tag{1}$$

$$V_{qs} = R_s I_{qs} + \frac{d\Phi_{qs}}{dt} + \omega_s \Phi_{\mathrm{ds}} \tag{2}$$

The components of the rotor voltage vector are given by following equations [9, 26, 27]:

$$\begin{cases} V_{dr} = R_r I_{dr} + \dfrac{d\Phi_{dr}}{dt} - \omega_r \Phi_{\mathrm{qr}} & (3) \\ V_{qr} = R_r I_{qr} + \dfrac{d\Phi_{qr}}{dt} + \omega_r \Phi_{\mathrm{dr}} & (4) \end{cases}$$

The equations of stator flux vector components [9, 26-28]:

$$\begin{cases} \Phi_{ds} = L_s I_{ds} + M I_{dr} & (5) \\ \Phi_{qs} = L_s I_{qs} + M I_{qr} & (6) \end{cases}$$

The equations of the rotor flux vector components [9, 26-28]:

$$\begin{cases} \Phi_{dr} = L_r I_{dr} + M I_{ds} & (7) \\ \Phi_{qr} = L_r I_{qr} + M I_{qs} & (8) \end{cases}$$

The electromagnetic torque equation [9, 26-28]:

$$C_e = p\frac{M}{L_s}\left(\Phi_{ds} I_{qr} - \Phi_{qs} I_{qr}\right) \tag{9}$$

The mechanical equation [9, 26-28]:

$$C_m = C_r + J\frac{d\Omega}{dt} + f\Omega \tag{10}$$

where:

V_{ds}, V_{qs}: stator voltages along the axis d and q.

V_{dr}, V_{qr}: rotor voltages along the axis d and q.
I_{qs}, I_{ds}: stator currents along the axis d and q.
I_{qr}, I_{dr}: rotor currents along the axis d and q.
Φ_{qs}, Φ_{ds}: stator fluxes along the axis d and q.
Φ_{qr}, Φ_{dr}: rotor fluxes along the axis d and q.
R_s, R_r: winding resistance of stator and rotor per phase.
L_s, L_r: cyclic inductances of stator and rotor.
ω_s, ω_r: stator and rotor angular velocities.
M: cyclic mutual inductance between stator and rotor.
p: number of pole pairs.
C_r: resistant torque.
f: viscous friction coefficient.
J: moment of inertia.

2.1 State space model of DFIG

Before applying robust control synthesis of LQG by LMI approach, we must describe the system model into state space.

We will first develop the basic principle of our control loop, illustrated in the synoptic diagram of Figure 2, which is an element of a controlled system, the regulator seeks to minimize the tracking error "e", i.e. the difference between the set point value of the stator voltages "r: Vds_ref, Vqs_ref" and the measured output quantities of the stator voltages "y: Vds, Vqs", the controller then generates a control signal consisting of the stator currents and voltages "u: Idr, Iqr, Vdr, Vqr" in order to maintain the stator voltages at 220V and the frequency at 50Hz, despite the influences of disturbances, power grid consumption variations, and wind speed changes.

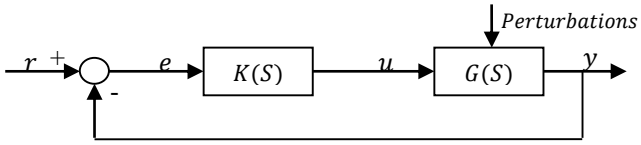

Figure 2. Feedback control of the perturbed aero-generator

where: K and G are respectively the robust controller and the Aero-generator.

The signals are:

The reference signal *'r'* is the stator voltage vector $\left[V_{ds\_ref}\ V_{qs\_ref}\right]'$.

The control signal *'u'* is a combined vector of the stator currents and the rotor voltages we can be written: $\left[I_{ds}\ I_{qs}\ V_{dr}\ V_{qr}\right]'$.

The measured output signal *'y'* is the stator voltage vector $\left[V_{ds}\ V_{qs}\right]'$.

The error signal *'e'* is the difference between the reference signal and the measured output signal.

Perturbations: are the variations in the electrical network consumption and in the wind speed.

In steady state the stator currents are constant, in addition their negative values must be eliminated in order to balance the heating in the stator windings [29], can be described by the following equation:

$$\frac{dI_{qs}(t)}{dt} = \frac{dI_{ds}(t)}{dt} = 0 \tag{11}$$

By combining the previous Eqns. (5)-(8) with (11), we obtain:

$$\begin{cases} \dfrac{d\varphi_{ds}}{dt} = \dfrac{M}{L_r}\dfrac{d\varphi_{dr}}{dt} & (12) \\ \dfrac{d\varphi_{qs}}{dt} = \dfrac{M}{L_r}\dfrac{d\varphi_{qr}}{dt} & (13) \end{cases}$$

We take the manipulation of the previous Eqns. (1)-(8) and combining them with Eqns. (12) and (13), and choosing the rotor-flux vector as a state vector $x = \left[\Phi_{\mathrm{dr}}\ \Phi_{\mathrm{qr}}\right]'$, we then get the following state space model (14):

$$\begin{cases} \dot{x} = Ax + Bu \\ y = Cx + Du \end{cases} \tag{14}$$

where:

$$A = \begin{bmatrix} \dfrac{-R_r}{L_r} & \omega_r \\ -\omega_r & \dfrac{-R_r}{L_r} \end{bmatrix};\ B = \begin{bmatrix} \dfrac{R_r.M}{L_r} & 0 & 1 & 0 \\ 0 & \dfrac{R_r.M}{L_r} & 0 & 1 \end{bmatrix};$$

$$C = -\frac{M}{L_r}.\begin{bmatrix} \dfrac{R_r}{L_r} & \omega \\ -\omega & \dfrac{R_r}{L_r} \end{bmatrix};$$

$$D = \begin{bmatrix} R_s + \dfrac{M^2}{{L_r}^2}.R_r & -\sigma.L_s.\omega_s & \dfrac{M}{L_r} & 0 \\ \sigma.L_s.\omega_s & R_s + \dfrac{M^2}{{L_r}^2}.R_r & 0 & \dfrac{M}{L_r} \end{bmatrix}.$$

We consider: $\omega = \omega_s - \omega_r$, is the rotor speed and $\sigma = 1 - \frac{M^2}{L_S.L_r}$, is the dispersion coefficient.

The internal representation of the state space (14) is given by the Figure 3.

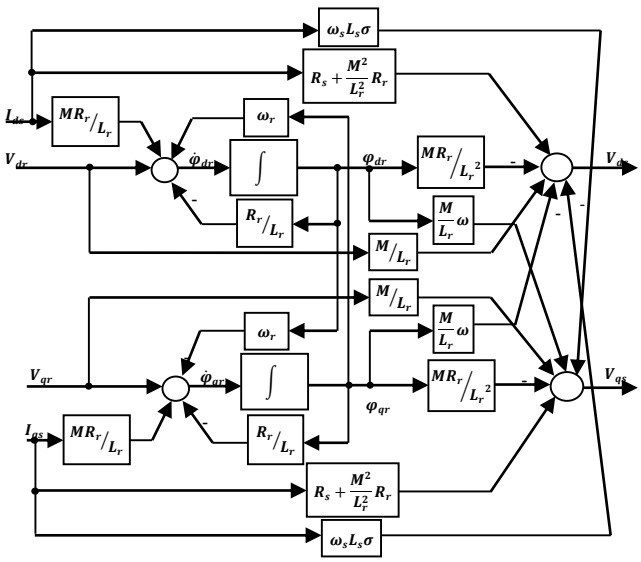

Figure 3. Internal model representation

where, the nominal parameters of the DFIG are given in the following Table 1:

Table 1. Nominal parameters of the DFIG

Parameter	Value	Unit	Parameter	Value	Unit
R_s	0,445	Ω	M	0,034	H
R_r	0,19	Ω	ω_s	$100.\pi$	rad/s
L_s	0,07	H	ω_r	148,70	rad/s
L_r	0,0213	H			

By substituting these numerical values in the state space equations of the DFIG (14), the following model is obtained:

$$A = \begin{bmatrix} -8{,}92 & 148{,}7 \\ -148{,}7 & -8{,}92 \end{bmatrix}; B = \begin{bmatrix} 0{,}3033 & 0 & 1 & 0 \\ 0 & 0{,}3033 & 0 & 1 \end{bmatrix}$$

$$C = \begin{bmatrix} -14{,}24 & -264{,}1 \\ 264{,}1 & -14{,}24 \end{bmatrix}$$

$$D = \begin{bmatrix} 0{,}9291 & -4{,}941 & 1{,}596 & 0 \\ 4{,}941 & 0{,}9291 & 0 & 1{,}596 \end{bmatrix}$$

The unit step response of the DFIG in nominal operating regime is shown in the following Figure:

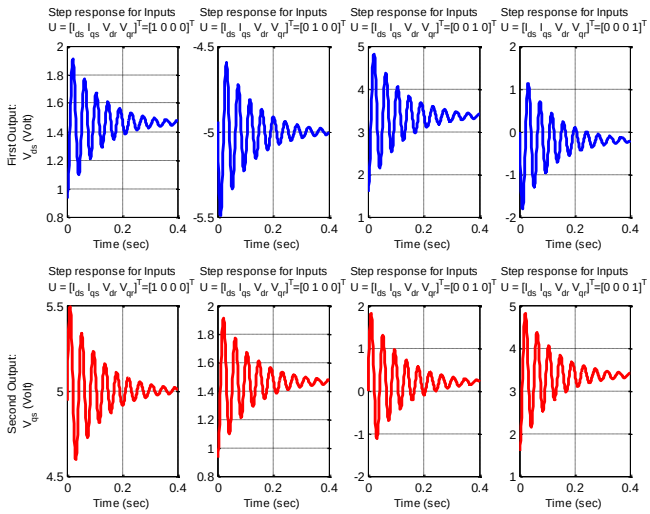

Figure 4. Open loop step responses of DFIG

From Figure 4, we see that the system outputs oscillate at the same frequency which varies as a function of the rotor rotational speed, but the amplitude of each output is different and gradually decreasing to a constant value (under-damped response) because of the coupling.

2.2 Transfer matrix model of DFIG

The Process (DFIG) can be represented by the following transfer matrix:

$$G(s) = C.(s.I + A)^{-1}.B + D \qquad (15)$$

$$\Rightarrow G(s) = \begin{bmatrix} G_{11}(s) & G_{12}(s) & G_{13}(s) & G_{14}(s) \\ G_{21}(s) & G_{22}(s) & G_{23}(s) & G_{24}(s) \end{bmatrix} \qquad (16)$$

$$G_{11}(s) = \frac{0{,}929\ (s^2\ +\ 13{,}19\,s\ +\ 3{,}497\,.10^4)}{(s^2\ +\ 17{,}84\,s\ +\ 2{,}219\,.10^4)}$$

$$G_{12}(s) = \frac{-4{,}941\ (s^2\ +\ 34{,}05\,s\ +\ 2{,}247.10^4)}{(s^2\ +\ 17{,}84\,s\ +\ 2{,}219\,.10^4)}$$

$$G_{13}(s) = \frac{1{,}596\ (s^2\ +\ 8{,}92\,s\ +\ 4{,}672\,.10^4)}{(s^2\ +\ 17{,}84\,s\ +\ 2{,}219\,.10^4)}$$

$$G_{14}(s) = \frac{-264{,}113\ (s + 16{,}94)}{(s^2\ +\ 17{,}84\,s\ +\ 2{,}219\,.10^4)}$$

$$G_{21}(s) = \frac{4{,}941\ (s^2\ +\ 34{,}05\,s\ +\ 2{,}247.10^4)}{(s^2\ +\ 17{,}84\,s\ +\ 2{,}219\,.10^4)}$$

$$G_{22}(s) = \frac{0{,}929\ (s^2\ +\ 13{,}19\,s\ +\ 3{,}497\,.10^4)}{(s^2\ +\ 17{,}84\,s\ +\ 2{,}219\,.10^4)}$$

$$G_{23}(s) = \frac{264{,}113\ (s + 16{,}94)}{(s^2\ +\ 17{,}84\,s\ +\ 2{,}219\,.10^4)}$$

$$G_{24}(s) = \frac{1{,}596\ (s^2\ +\ 8{,}92\,s\ +\ 4{,}672\,.10^4)}{(s^2\ +\ 17{,}84\,s\ +\ 2{,}219\,.10^4)}$$

The DFIG has two complex conjugate modes, are given by:

$$\det(s\,I_2 - A) = 0 \Rightarrow \begin{cases} s_1 = -8{,}92 - j\,148{,}7 \\ s_2 = -8{,}92 + j\,148{,}7 \end{cases};$$

The following figure representats the process principal gains.

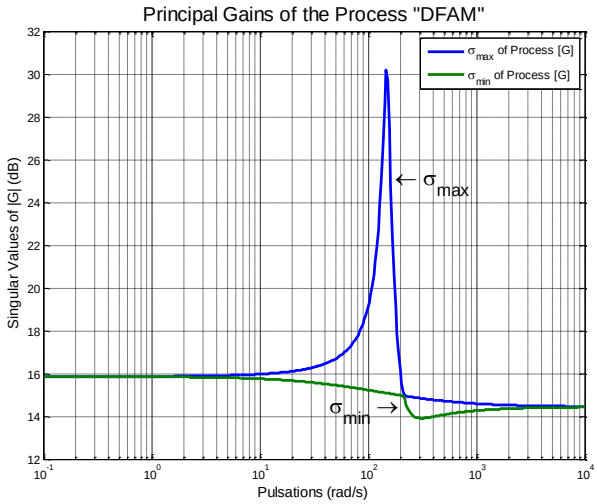

Figure 5. Principal Gains of the "DFIG" G(s)

From Figure 5, we remark that the gap between the maximum and minimum principal gain of the process is important in medium frequencies because of its two complex conjugate modes, which explains the coupling of the DFIG confirmed in the Figure 4, where the control becomes difficult in this case Frequency range.

3. ROBUSTNESS CONCEPTS

It is necessary to recall the robustness notions of feedback system, Figure 6, in the frequency domain.

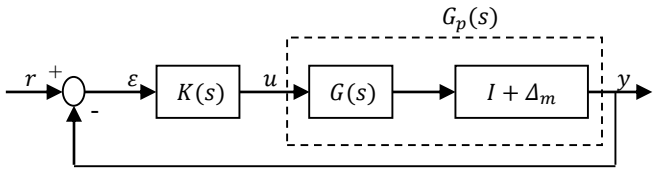

Figure 6. System control configuration with output multiplicative perturbation

The system considered is shown in Figure 6, where: $K(s)$ and $G_p(s)$, the robust controller and the perturbed process, respectively.

$\Delta_m(s)$, Represents the output multiplicative uncertainties of

the process including all perturbations [12, 30], mentioned in the previous sections, which act on the plant.

Thus, the DFIG is subject to the following parametric variations which will cause important dynamic variations:

- Rotor and stator resistance uncertainties 'ΔR_r and ΔR_s' vary by 50% around their nominal values.
- Rotor and stator inductance uncertainties 'ΔL_r and ΔL_s' vary by 20% around their nominal values.
- Rotor angular velocity uncertainty '$\Delta\omega_r$' vary by 15% around its nominal value.

From where the following relationships can be written:

$$G_p(s) = [I + \Delta_m(s)].G(s) \tag{17}$$

From (14) we will have:

$$\Delta_m(s) = \big(G_p(s) - G(s)\big).G^{-1} \tag{18}$$

We introduce the notion of maximum singular values denoted ' $\overline{\sigma}$ ' in relation (18), to quantify the output multiplicative uncertainties of the process "Aero-generator", which gives:

$$\overline{\sigma}[\Delta_m(j\omega)] = \overline{\sigma}\big(\big[G_p(j\omega) - G(j\omega)\big].G^{-1}(j\omega)\big) \tag{19}$$

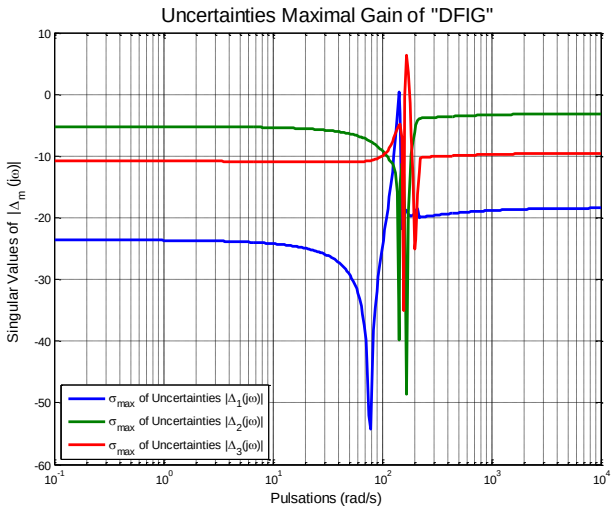

Figure 7. Process uncertainties ($\Delta_m(s)$)

From Figure 7 we show plot of the relationship (19), it is found that the maximum singular values of the output multiplicative uncertainties of the Aero-generator are lower at the low frequencies whereas in the medium and high frequencies the uncertainties increase due to the disturbance effects [14].

It is also noted that there is a peak at the pulsation of 146,6 rad/s, which means that the process is strongly coupled at the medium frequencies

From where, the choice of the stability specification W_t is given by the following relation [12, 14]:

$$\overline{\sigma}[\Delta_m(j\omega)] \leq \overline{\sigma}[W_t(j\omega)] \quad \forall\, \omega \tag{20}$$

From the relation (20), the maximum singular values of the stability specification W_t represents the upper bound of the maximum singular values of the uncertainties; see Figure 8, therefore the stability specification in all frequency range is given by:

$$W_t(j\omega) = 0{,}9.\begin{bmatrix}(1 + j\ 0{,}023\omega) & 0\\ 0 & (1 + j\ 0{,}023\omega)\end{bmatrix} \tag{21}$$

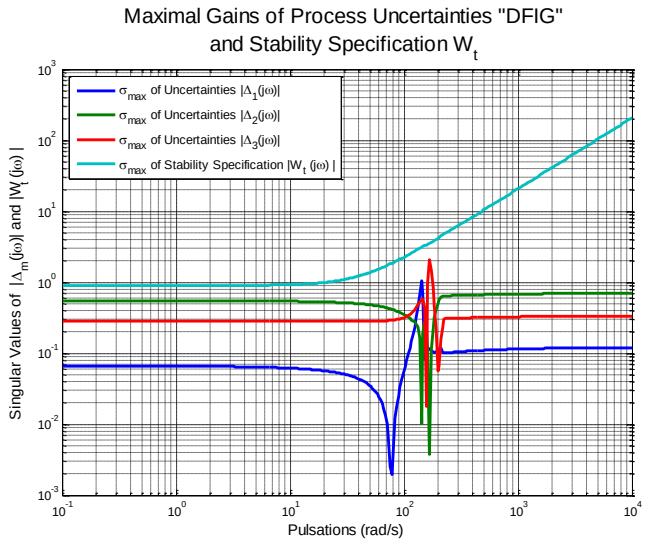

Figure 8. Choice of the stability specification $W_t(s)$

3.1 The robustness conditions on stability and performances

The robustness conditions on the stability and the performances corresponding to the output multiplicative uncertainties (18) are respectively [12, 31]:

$$\overline{\sigma}[T(j\omega).W_t(j\omega)] < 1 \tag{22}$$

$$\overline{\sigma}\big[S(j\omega).W_p(j\omega)\big] \leq 1 \tag{23}$$

Is the nominal process transfer matrix defined by:

$$T(j\omega) = G(j\omega).K(j\omega).[I + G(j\omega).K(j\omega)]^{-1} \tag{24}$$

It represents the transfer matrix between the reference *r* and the output *y*; it reflects the measurement noises influence on the output and the error ε [14, 31].

And $S(j\omega)$ is the sensitivity matrix defined by:

$$S(j\omega) = [I + G(j\omega).K(j\omega)]^{-1} \tag{25}$$

It represents the transfer matrix between the reference r and the error ε, it reflects the perturbations influence on the output y and on the error ε [14, 31].

$T(j\omega)$ and $S(j\omega)$ are complementary:

$$S(j\omega) + T(j\omega) = I \tag{26}$$

The relation (26) recalls the stability-performance dilemma of a system i.e. any stability adjustment results in performances adjustment [14, 31].

$W_p(j\omega)$: Represents the weighting matrix function, is chosen in order to satisfy the performance specifications so as to ensure the precision and rapidity of the closed-loop system.

Our choice is obtained as follows:

$$W_p(j\omega) = \begin{bmatrix} \dfrac{(1 + j\ 0{,}05\omega)}{j\ 0{,}05\omega} & 0 \\ 0 & \dfrac{(1 + j\ 0{,}05\omega)}{j\ 0{,}05\omega} \end{bmatrix} \quad (27)$$

The singular values of the matrix of the specifications on the performances are shown in Figure 9, we observe that they are too important at low frequencies and this guarantee good precision, i.e. zero static error, integrator effect (integral action).

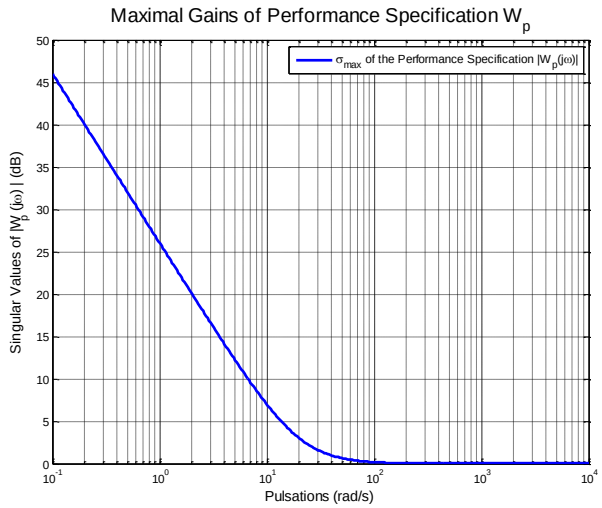

Figure 9. Choice of the performance specification $W_p(s)$

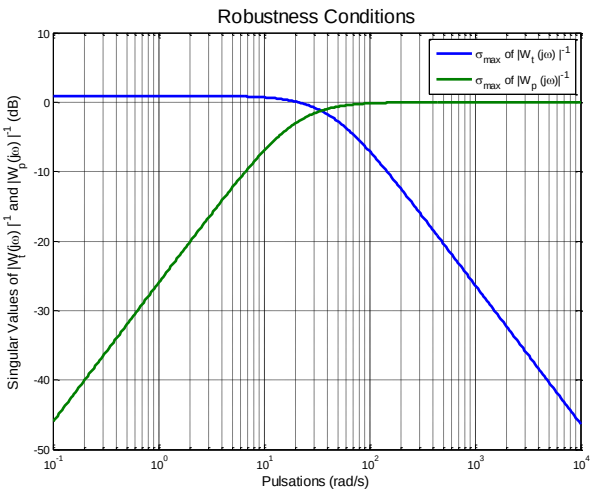

Figure 10. Robustness conditions of process "DFIG"

According to Figure 10, the robustness conditions are set such that the chosen specification functions must be the upper bounds of the loop nominal operating regime in order to guarantee stability against the influences of the model uncertainties by the rejection of disturbances effects in low frequencies and to ensure desired performances with the rejection of measurement noises in high frequencies.

3.2 The stability robustness condition

Suppose that the nominal process $G(s)$ is stable (with $\Delta_m(s) = 0$), then the perturbed regime is also stable [12] if and only if the robustness condition on stability is satisfied [12, 14, 31]:

$$\overline{\sigma}[T(j\omega)] < \overline{\sigma}[W_t(j\omega)]^{-1} \quad (28)$$

3.3 The performance robustness condition

If the robustness condition on the stability (28) is respected, then the disturbed regime ensures the desired performances (without overshoot, settling time and precision) in closed loop if and only if the following robustness condition on the performances is satisfied [12, 31, 32]:

$$\overline{\sigma}[S(j\omega)] \leq \overline{\sigma}[W_p(j\omega)]^{-1} \quad (29)$$

4. THE ROBUST LQG CONTROL

In this section we present the LQG control and its robustness properties, it is an optimization method which consists in designing a robust controller, in the internal loop consisting of a Kalman Filter in order to estimate the system state and the latter is looped by a state feedback control "LQ" [5].

First of all, if the system type is zero, an additional integrator is added to the process where it becomes an augmented process so that the steady-state error is eliminated and ensures the precision of the LQG controller [13].

The augmented process becomes:

$$\begin{cases} \dot{x}(t) = A_a x(t) + B_a u(t) \\ y(t) = C_a x(t) + D_a u(t) \end{cases} \quad (30)$$

With: $A_a = \begin{bmatrix} A & 0_{n\times l} \\ C & 0_{l\times l} \end{bmatrix}$; $B_a = \begin{bmatrix} B \\ D \end{bmatrix}$; $C_a = [0_{l\times n} \quad I_{l\times l}]$; $D_a = 0_{l\times m}$;

where: m is the inputs number, l is the outputs number and n is the states number of the system.

4.1 Position of the LQG problem

In most cases, the system state representation does not have a complete knowledge of the state vector; however, the application of the LQ control by state feedback requires knowledge of all its state variables. For this purpose, we first have to reconstruct all the non-measurable state variables (and / or with noises) of the process by introducing a state estimator "KALMAN Filter" Then by applying to the estimated state variables the state feedback control LQ (Figure 11) which minimizes a stochastic quadratic criterion with the fundamental hypothesis is that the noises are of a Gaussian white nature, this problem is known as Gaussian Quadratic Linear LQG [5, 33].

We add two Gaussian white noises to our augmented process of the aero-generator, which leads to a stochastic process, represented in the following state space:

$$\begin{cases} \dot{x}(t) = A_a x(t) + B_a u(t) + w(t) \\ y(t) = C_a x(t) + v(t) \end{cases} \quad (31)$$

With $v(t)$ and $\omega(t)$ are independent centered Gaussian noises with covariance matrix [5]:

$$E[v(t)v'(t+\tau)] = V\,\delta(t) > 0,$$
$$E[w(t)w'(t+\tau)] = W\,\delta(t) > 0,$$
$$\text{and } E[w(t)v'(t+\tau)] = 0$$

This LQG control problem consists to minimize the following quadratic criterion [5]:

$$J = E\left[\int_0^{\infty} (x'(t)\, Q\, x(t) + u'(t) R\, u(t))dt\right] \qquad (32)$$

With: $R = R' > 0$ *and* $Q = Q' > 0$ two weighting matrices

The solution of this LQG control problem is obtained by applying the separation theorem [6, 7, 8], divides the problem into two distinct parts.

- By using a Kalman Filter as an observer to reconstruct the estimated values $\hat{x}$ of the system state *x* (provided that the triplet $(C,\ A, W^{1/2})$ is detectable [25, 34]), in the sense of the minimum error variance, which is unbiased, i.e. the estimation error $\varepsilon(t) = x(t) - \hat{x}(t)$ is independent of the system state *x*(*t*) (31), where it vanishes under steady state [33, 35].
- By applying to the estimated state *x* the state feedback control $u(t) = -K\hat{x}(t)$ and considering this estimated state as if the exact state *x* of the process [33], that is, suppressing *v*(*t*) and *w*(*t*) of the state equation (31) and the mathematical expectation "E" in criterion (32).
  Where, *K* is calculated by solving the deterministic optimal control problem (LQ) which stabilizes the system. Hence, the triplet $(A, B, Q^{1/2})$ must be stabilizable [25, 34].

Then, once both parties are resolved, their solutions are combined to form a single solution to the complete problem (Figure 11).

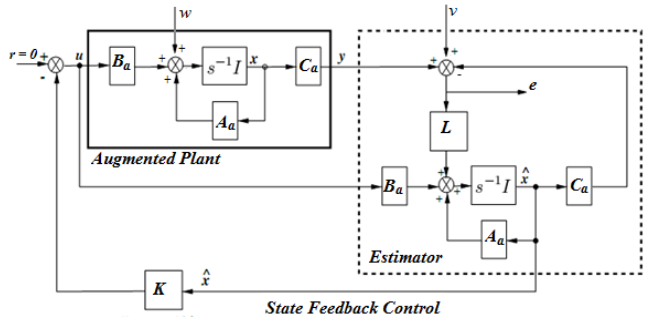

Figure 11. Structure of the LQG Control, with the Augmented Plant is considered strictly proper (D_a = 0)

1.1. Formulation of the Problem LQG by applying the Separation Theorem

Step 1: the reconstruction of the estimated state $\hat{x}$ by the Kalman Filter.

- *Principle of the Kalman Filter*

Let us now return to our stochastic process (uncertain system) represented in (31), whose:

$w(t)$: is an upper bound signal, that is, the process state *x*(*t*) does not evolve exactly as deterministic model predicts (30), it represents the external perturbations acting on the process (wind speed variations on the aero-generator blades, electrical energy consumption via the electrical network directly connected to DFIG) and also the modeling errors or uncertainties (parametric variations of the DFIG because of the physical phenomena, the gap between the non-linear model and the tangent linear model due to linearization, ...).

$v(t)$: represents measurement noise related to the sensors used.

Kalman Estimator (see Figure 11) is a dynamic system with two inputs, u signal control (process input) and y measurement (process output), and an output which is the process estimated state $\hat{x}(t)$ given by the following equation of Kalman Filter (Kalman State Estimator):

$$\dot{\hat{x}}(t) = \left(A_a\hat{x}(t) + B_a u(t)\right) + L.e(t) \qquad (33)$$

$$\text{where: } e(t) = y(t) - \hat{y}(t) \text{ and } \hat{y}(t) = C_a\,\hat{x}(t) \qquad (34)$$

L: Estimator (Kalman) gain matrix.

Substituting (34) into (33), we will have for the system described in (30):

$$\dot{\hat{x}} = A_a\hat{x}(t) + B_a u(t) + L\, C_a(x - \hat{x}) \qquad (35)$$

Assumptions: 1- the (A_a, C_a) pair is detectable,
2- *w* and *v*: Centered and independent white Gaussian noises.

We know that the estimation error is given by:

$$\begin{aligned} \varepsilon(t) = x(t) - \hat{x}(t) \Rightarrow \dot{\varepsilon}(t) = \dot{x}(t) - \dot{\hat{x}}(t) \\ \Rightarrow \dot{\varepsilon}(t) = (A_a - LC_a)\left(x(t) - \hat{x}(t)\right) \\ \Rightarrow \dot{\varepsilon}(t) = (A_a - LC_a)\varepsilon(t) \end{aligned} \qquad (36)$$

If the eigenvalues of $(A_a - LC_a)$ have a strictly negative real part then the Estimator is asymptotically stable and the estimation error tends to zero, so the Estimator is constructed.

Step 2: Application of the state feedback control $u(t) = -K\hat{x}(t)$ on the estimated state.

Before applying the LQ control, the estimator realized in the first step (Kalman filter) must be used to perform the feedback control on the estimated state.

Thus, we can rewrite the state equations of the stochastic process (31) in the form:

$$\begin{cases} \dot{x}(t) = A_a x(t) + B_a u(t) + w(t) \\ \dot{\hat{x}}(t) = A_a\hat{x}(t) + B_a u(t) + LC_a(x - \hat{x}) + Lv(t) \end{cases} \qquad (37)$$

Let us set $u(t) = -K\hat{x}(t)$, from the state equations (37), it comes:

$$\begin{cases} \dot{x}(t) = A_a x(t) - B_a K\hat{x}(t) + w(t) & (38.a) \\ \dot{\hat{x}}(t) = A_a\hat{x}(t) - B_a K\hat{x}(t) + \cdots \\ \quad \ldots + LC_a\left(x(t) - \hat{x}(t)\right) + Lv(t) & (38.b) \end{cases}$$

We subtract (38.a) from (38.b) and substituting in the obtained equation by the relation of the estimation error vector $\varepsilon(t) = x(t) - \hat{x}(t)$, then we deduce the following equation for the evolution of the state estimation error:

$$\Rightarrow \dot{\varepsilon}(t) = (A_a - LC_a)\varepsilon(t) + w(t) - Lv(t) \qquad (39)$$

The new state representation can be put in the following modal form:

$$\begin{cases} \dot{x}(t) = A_a x(t) - B_a K(x(t) - \varepsilon(t)) + w(t) \\ \dot{\varepsilon}(t) = (A_a - LC_a)\varepsilon(t) + w(t) - Lv(t) \end{cases} \qquad (40)$$

$$\begin{aligned} \Rightarrow \begin{pmatrix} \dot{x}(t) \\ \dot{\varepsilon}(t) \end{pmatrix} = \begin{pmatrix} A_a - B_a K & B_a K \\ 0 & A_a - LC_a \end{pmatrix} \begin{pmatrix} x(t) \\ \varepsilon(t) \end{pmatrix} + \cdots \\ \ldots + \begin{pmatrix} I & 0 \\ I & -L \end{pmatrix} \begin{pmatrix} \omega(t) \\ v(t) \end{pmatrix} \end{aligned} \qquad (41)$$

From this modal representation (41), we notice that the state matrix $\begin{pmatrix} A_a - B_aK & B_aK \\ 0 & A_a - LC_a \end{pmatrix}$ is a triangular matrix, Its modes are the eigenvalues of the elements of the diagonal: $(A_a - B_aK)$ et $(A_a - LC_a)$ Are respectively the dynamics of the state feedback and the dynamics of the estimator which are separated That is to say that the eigenvalues of the control are adjusted by the state feedback gain matrix K independently of the eigenvalues of the estimator which are adjusted by the matrix L of the estimator, it is the separation principle.

Step 3: The Separation of the quadratic criterion to be minimized for the LQG control.

Taking the chosen estimation error vector $\varepsilon(t) = x(t) - \hat{x}(t)$, implies that the state vector is given by the following relation:

$$x(t) = \varepsilon(t) + \hat{x}(t) \tag{42}$$

If this Eq. (42) is combined with criterion LQG (32), we obtain:

$$J_{LQG} = E\left[\int_0^\infty \Big(\big(\varepsilon(t) + \hat{x}(t)\big)' Q \,\big(\varepsilon(t) + \hat{x}(t)\big) + \cdots \right. \\ \left. \cdots + \big(u'(t)\, R\, u(t)\big)\Big) dt\right] \tag{43}$$

$$\Rightarrow J_{LQG} = E\left[\int_0^\infty (\varepsilon'(t) Q\, \varepsilon(t) + \hat{x}'(t) Q\, \hat{x}(t) + \cdots \right. \\ \left. \ldots + 2\,\hat{x}'(t)\, Q\, \varepsilon(t) + u'(t)\, R\, u(t)\big) dt\right] \tag{44}$$

Since $\hat{x}(t)$ is not random it comes:

$$J_{LQG} = \int_0^\infty \big(\hat{x}'(t)\, Q\, \hat{x}(t) + u'(t)\, R\, u(t)\big) dt + \cdots \\ \ldots + E\left[\int_0^\infty \Big(\varepsilon'^{(t)} Q\, \varepsilon(t)\Big)\, dt\right] + \cdots \\ \ldots + \left[2\int_0^\infty \hat{x}'^{(t)} Q\, E[\varepsilon(t)] dt\right] \tag{45}$$

$$\Rightarrow J_{LQG} = J_{LQ} + E\left[\int_0^\infty \big(\varepsilon'(t)\, Q\, \varepsilon(t)\big) dt\right] \tag{46}$$

where: $E[\varepsilon(t)] = 0$ because ε is a centered random vector (zero mean).

Hence the LQG control criterion is composed in two parts $J_{LQG} = J_{LQ} + J_e$ (separation principle).

$$J_{LQ} = \int_0^\infty \big(\hat{x}'(t)\, Q\, \hat{x}(t) + u'(t)\, R\, u(t)\big) dt \tag{47}$$

J_{LQ}: It is a quadratic criterion LQ type applied to the estimated state $\hat{x}(t)$ of the Kalman filter.

Therefore the Kalman filter must be designed so that the quantity $E\left[\int_0^\infty \big(\varepsilon'(t)\, Q\, \varepsilon(t)\big) dt\right]$ is the smallest possible value.

$$J_e = E\left[\int_0^\infty \varepsilon'(t) Q\, \varepsilon(t) dt\right] = tr[QE\{\varepsilon(t)\varepsilon'(t)\}] \tag{48}$$

The minimum of the criterion (48) is obtained by the estimator (Kalman) gain matrix *L*, so that the estimation error covariance matrix, $P_f(t) = E\{\varepsilon(t)\varepsilon'(t)\}$, is the minimum [33, 35].

4.2 Reformulation of the LQG problem by the LMI approach

The problem can be rewritten as an LMI problem while considering the estimator problem as a LQ control problem because of the existing correspondences between the control and the estimator Dual / primal, Verified by Kalman (1960) [36]. We assume that the system is observable and (36) give the dynamics of the error between the measured state and the estimated state:

$$\dot{\varepsilon}(t) = (A_a - LC_a)\varepsilon(t)$$

The objective is to determine the gain of the Estimator '*L*' so that the poles of $(A_a - LC_a)$ are stable. If by transposing the expression of the dynamic matrix $(A_a - LC_a)$, it comes that this objective is equivalent to determine a state feedback for a fictitious system (A_a', C_a').

Indeed, then:

$$det\big(sI - (A_a - LC_a)\big) = det\big(sI - (A_a' - C_a'L')\big)$$

which implies determine the fictitious state feedback with gain matrix K for the fictitious state-space system (A_a', C_a') and we calculate the estimator gain by: $L = K'$.

The primal / dual correspondences are summarized in the following Table 2 [33]:

Table 2. Primal / Dual correspondences between LQ control and Estimator

Primal	Dual
A_a	A_a'
B_a	C_a'
C_a	B_a'
Q	W
R	V
K	L'
P	P_f

4.3 Determination of the state feedback gain matrix K by using LMI-EVP problem

The formulation of this LQ control problem by LMI-EVP problem solving is based using the method given by [16, 37].

- *Position of the LQ control Problem by LMI approach*

We consider the linear time-invariant stochastic system described by (31), the LQ control problem consists to find a gain matrix *K* such that the quadratic criterion (32) is minimum, which gives:

$$\min_K J_{LQ} = \min_K \left[\int_0^\infty \big(\hat{x}'(t) Q\, \hat{x}(t) + u'(t) R\, u(t)\big) dt\right] \tag{49}$$

Let us put the state feedback control law of the form $u(t) = -K\hat{x}(t)$, we consider that the estimated state $\hat{x}(t)$ as being the exact measure of state $x(t)$ of the deterministic case, whence the criterion (49) becomes:

$$\min_K J_{LQ} = \min_K \left[\int_0^\infty x'(t)Q\,x(t) + \cdots \right. \\ \left. \cdots + x'(t)K'R^{1/2}R^{1/2}Kx(t)dt \right] \quad (50)$$

We introduce the Trace operator in criterion (50), we will have:

$$\min_K J_{LQ} = \min_K \left[\int_0^\infty Tr(Q\,x(t)x'(t) + \cdots \right. \\ \left. \cdots + R^{1/2}\,K\,x(t)x'(t)K'\,R^{1/2})dt \right] \quad (51)$$

We know that: $P(t) = \int_0^\infty x(t)x'(t)dt$ is the solution of the Lyapunov equation where: $P(t) = P'(t) > 0$, Then criterion (51) becomes [16]:

$$\min_{P,K} Tr\left[(Q\,P + R^{1/2}\,K\,PK'\,R^{1/2})\right] \quad (52)$$

The system (31) is asymptotically stable in Closed-Loop by state feedback law $u(t) = -K\,x(t)$ if and only if all the eigenvalues of $(A_a - B_aK)$ have a strictly negative real part, i.e. there is no pole on the imaginary axis.

To prove the asymptotic stability, we will apply the Lyapunov stability theorem:

Let the Lyapunov function $V(x) = x'Px,\ \forall x \neq 0$ where $P = P' > 0$ is the solution of the Lyapunov equation whose necessary stability condition is given by the research of [38]:

$$\frac{dV(x)}{dt} < 0 \quad (53)$$

$$\Rightarrow x'\big((A_a - B_aK)'P + P(A_a - B_aK)\big)x\ < 0, \forall\, x \neq 0 \quad (54)$$

$$\text{where: } \big((A_a - B_aK)'P + P(A_a - B_aK)\big) = -I_n \quad (55)$$

The inequality (54) is bilinear (BMI), because it includes the multiplication of the variables P and K, by changing the variable $x = P^{-1}\tilde{x}$, we obtain:

$$\Rightarrow\ \tilde{x}'(P^{-1}(A_a - B_aK)' + (A_a - B_aK)P^{-1})\tilde{x}\ < 0, \quad \forall\, x \neq 0 \quad (56)$$

Similarly, the inequality (56) is not affine (non-convex) due to apparition of the multiplicative term P.K, so we need to introduce a new variable, see the research of [16], $Y = KS$ where $S = P^{-1}$ in the inequality (56) to convert it from BMI into LMI, we will have:

$$\Rightarrow \tilde{x}'\big(S\,A_a' - (KP^{-1})'B_a' + A_aS - B_a(KP^{-1})\big)\tilde{x} < 0, \quad \forall\, x \neq 0 \quad (57)$$

$$\Rightarrow \tilde{x}'(S\,A_a' - Y'B_a' + A_aS - B_aY)\tilde{x}\ < 0, \forall\, x \neq 0 \quad (58)$$

This condition can be formulated into the following LMI optimization problem:

The controllable system (31), is stable if and only if

$$(A_aS + S\,A_a' - Y'B_a' - B_aY) + I_n < 0, \\ with: S = S' > 0\ is\ feasible \quad (59)$$

From (52) and (59), the gain matrix K by state feedback is calculated by minimizing the following LMI expression:

$$\min_{S,K} Tr\left[(Q\,S + R^{1/2}\,K\,SK'\,R^{1/2})\right] \\ \text{Subject to: } A_aS + S\,A_a' - B_aY - Y'B_a' + I_n < 0, \\ S = S' > 0 \quad (60)$$

With: $K = Y.S^{-1}$, where: S is Lyapunov Matrix.
is equivalent to:

$$\min_{S,K} Tr\left[(Q\,S + R^{1/2}\,(K\,S)S^{-1}(K\,S)'\,R^{1/2})\right] \\ \text{Subject to: } A_aS + S\,A_a' - B_aY - Y'B_a' + I_n < 0, \\ S = S' > 0 \quad (61)$$

Replacing the new variable $Y = KS$ in the cost function of expression (61), we find

$$\min_{S,Y} \left[Tr(Q\,S) + Tr\left(R^{\frac{1}{2}}\,Y\,S^{-1}\,Y'\,R^{\frac{1}{2}}\right)\right] \\ \text{Subject to: } A_aS + S\,A_a' - B_aY - Y'B_a' + I_n < 0, \\ S = S' > 0 \quad (62)$$

The term $Tr(R^{1/2}\,Y\,S^{-1}\,Y'\,R^{1/2})$ present in the objective function is nonlinear; it must be changed by a second auxiliary variable X [16].

$$Tr\left(R^{\frac{1}{2}}\,Y\,S^{-1}\,Y'\,R^{\frac{1}{2}}\right) = \\ \begin{cases} \min_X Tr(X) \\ \text{Subject to: } X > \left(R^{\frac{1}{2}}\,Y\,S^{-1}\,Y'\,R^{\frac{1}{2}}\right) \end{cases} \quad (63)$$

In order to decompose the inequality (63), we must use the Schur complement as follows, for more details see the researches of [17,39]:

$$X > \left(R^{\frac{1}{2}}\,Y\,S^{-1}\,Y'\,R^{\frac{1}{2}}\right) \\ \Leftrightarrow \begin{bmatrix} X & R^{1/2}Y \\ Y'R^{1/2} & S \end{bmatrix} > 0 \quad (64)$$

This problem is equivalent to the eigenvalues problem. Finally, the Formulation of the state feedback control (LQ problem) into LMI approach is given by the following expression:

$$\min_{S,Y,X} Tr(Q\,S) + Tr(X) \\ \text{Subject to: } A_aS + S\,A_a' - B_aY - Y'B_a' + I_n < 0, \\ \begin{bmatrix} X & R^{1/2}Y \\ Y'R^{1/2} & S \end{bmatrix} > 0, \quad S > 0 \quad (65)$$

This is a LMI-eigenvalue problem (LMI-EVP), once this problem of the minimization under constraints is solved, the state feedback gain matrix of the LQ control is calculated by: $K = Y.S^{-1}$.

4.4 Determination of the Estimator Gain 'L' by using LMI-EVP problem

The summary of the Dual / primal correspondences between the LQ control and the Estimator given in Table 2, will allow us to directly express the optimality conditions of the estimator

(observer) gain matrix 'L' from those obtained for the control gain matrix K by the LMI approach expression (65):

$$\min_{P_f,Y,X} Tr(W\,P_f) + Tr(X_f)$$
$$\text{Subject to: } A_a'P_f + P_f A_a - Y_f C_a - C_a' Y_f{}' + I_n < 0, \quad \begin{bmatrix} X_f & V^{1/2}Y_f{}' \\ Y_f V^{1/2} & P_f \end{bmatrix} > 0, \quad P_f > 0 \tag{66}$$

This is an LMI-eigenvalue problem (LMI-EVP), once this minimization problem under constraints is solved, the Estimator Gain is calculated by: $L = P_f{}^{-1}.Y_f$.

4.5 LQG controller

From the dynamic equation of the Kalman filter (35) and the state feedback control law $u(t) = -K\,\hat{x}(t)$, the controller dynamics is given by:

$$\begin{cases} \dot{\hat{x}}(t) = (A_a - B_a K - LC_a)\hat{x}(t) + Ly(t) \\ u(t) = -K\,\hat{x}(t) \end{cases} \tag{67}$$

Thus, the state representation of the controller LQG can be rewritten by considering the tracking control law $U(s) = C(s).(Y_r(s) - Y(s))$ where $Y_r(s)$ is the set-point (Figure 12), he comes:

$$\begin{pmatrix} \dot{\hat{x}} \\ u \end{pmatrix} = \begin{pmatrix} (A_a - B_a K - LC_a) & -L \\ -K & 0 \end{pmatrix} \begin{pmatrix} \hat{x} \\ y_r - y \end{pmatrix} \tag{68}$$

where, the LQG controller transfer matrix is obtained by performing the following calculation:

$$C(s) = K(sI_n - A_a + B_a K + LC_a)^{-1} L \tag{69}$$

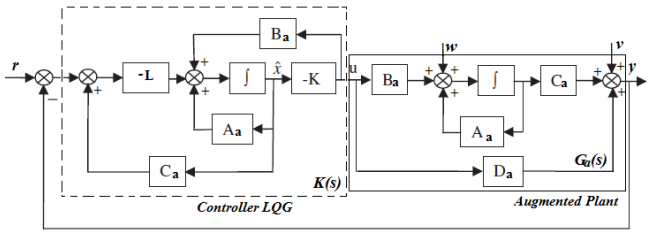

Figure 12. Dynamics of the LQG robust controller with augmented plant in the closed loop

5. SIMULATION RESULTS

The implementation of the LQG controller is realized using the Matlab / Simulink software according to the following functional diagram (Figure 13).

As indicated in the previous section that the LQG controller relies on the separation theorem, by using the estimated state $\hat{x}$ as if it were the exact measurement of the system state x "rotor fluxes" which requires adjusting the Kalman estimator by choosing variance matrices V and W; then adjusting the state feedback control (LQ) by choosing the weighting matrices Q and R to have a "good" state feedback.

5.1 Adjustment of variance matrices W and V

In order to obtain an observer to reconstruct (estimate) the state of the DFIG x "rotor fluxes", the choice of the noise variance matrices V and W of the Kalman estimator is given as follows:

$$\begin{cases} V = E\{v^T v\} = \sqrt{\alpha}.I_{m\times n} \\ W = E\{w^T w\} = \mathrm{C_a}^{\mathrm{T}}.\mathrm{C_a} \end{cases} \tag{70}$$

where: α is determined by "loop-shaping" to ensure the robust performance condition (29) to achieve performance objectives, that is, the singular maximum values of the performances specification function are an upper bound on the maximum singular values of the sensitivity function, Figure 14.

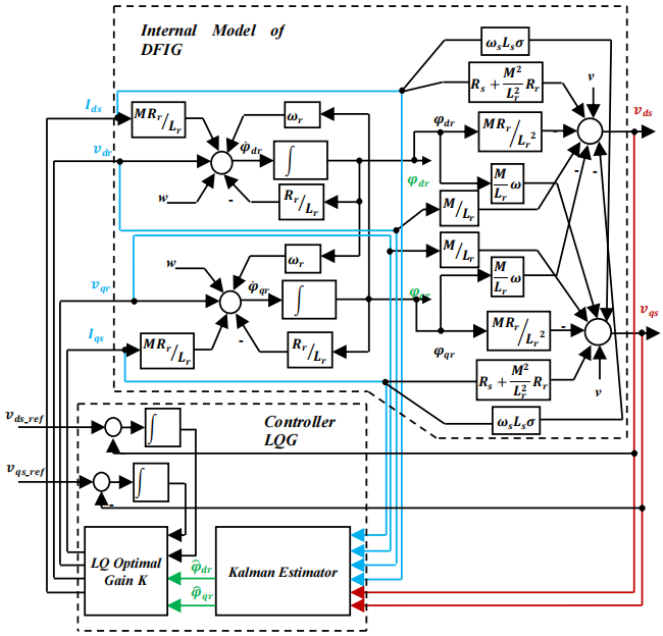

Figure 13. Functional diagram of the LQG controller with DFIG plant in feedback

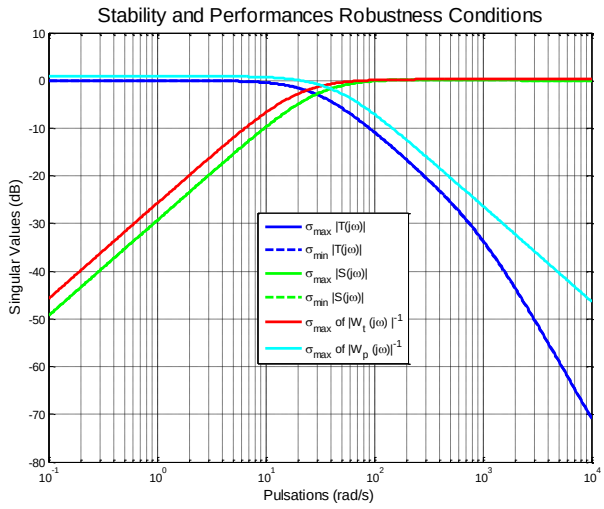

Figure 14. Principal gains of the stability and performances robustness conditions

5.2 Adjustment of the Q and R weighting matrices

To obtain a robust LQG controller, it must first be ensured that the relation of the robust stability condition is verified (28),

that is to say the maximum singular values of the complementary sensitivity function is bounded lower by the maximum singular values of the inverse multiplicative uncertainties function, Figure 14, to have a "good" state feedback, so for that we chose the weighting matrices Q and R of the quadratic criterion (32) in the following form:

$$Q = {C_a}^T C_a, and\ R = \sqrt{\rho}.I_{n\times n}$$

5.3 Results in frequency domain

According to Figure 14, it is observed that the robustness conditions are guaranteed, with a good margin of robustness in stability at High Frequencies, from where the values of parameters α and ρ are determined:

$$\alpha = 1{,}1\,.\,10^{-3}\ and\ \rho = 3.10^{-5}$$

5.4 Results in time domain

In this section, we will illustrate the results in the time domain. By applying a unit step signal to the DFIG input with the LQG controller in closed loop.

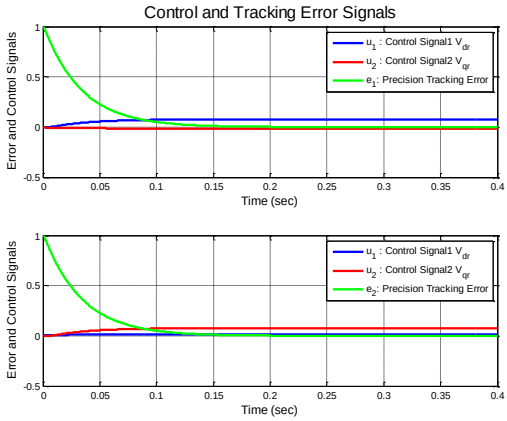

Figure 15. Signals of the control and tracking error

According to the Figure 15, we observe that the tracking error is reduced to zero and that the rotor voltages are low, which explains a minimization of the control energy.

The subsequent figures illustrate the step responses of the closed-loop control system for the nominal and disturbed operating regimes of the DFIG.

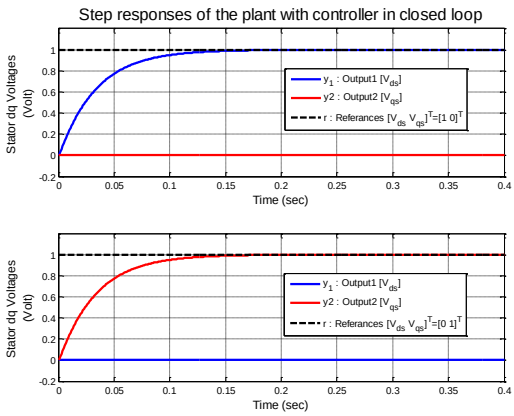

Figure 16. Temporal response of the LQG-controlled nominal plant "DFIG" in closed loop

In the Figure 16, we show that the output stator voltages reached the set-point without overshoot with a good settling time.

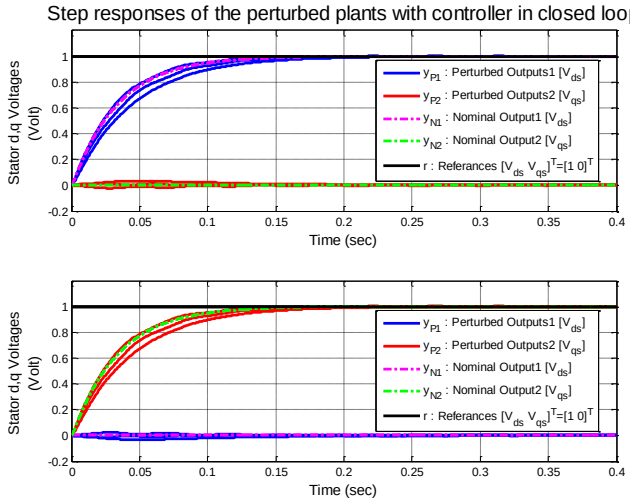

Figure 17. Temporal responses of the LQG-controlled uncertain DFIG plant (DFIG with disturbances)

Similarly, the Figure 17 shows that the output stator voltages of all disturbed DFIG plants reach the set-point without overshoot with a good settling time, the presence of a weak coupling is observed in transient response. In the following, the values of the set-point (rotor voltages) are varied successively at 100V, 380V and 220V in order to be able to visualize the amplitude follow-up control.

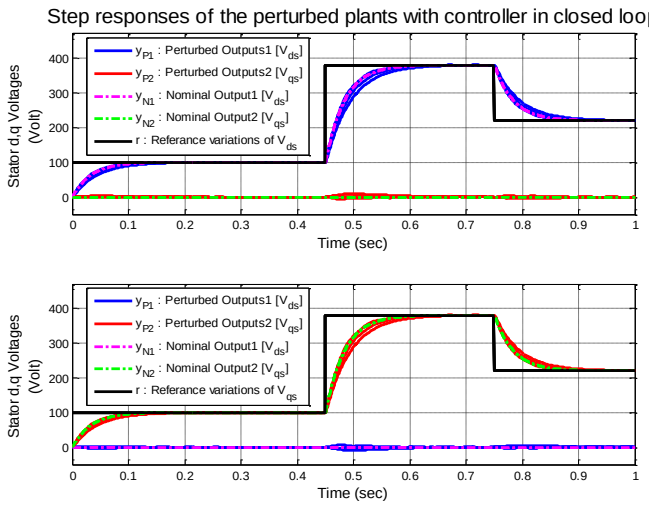

Figure 18. Step responses with reference tracking in the closed loop of the LQG-controlled uncertain "DFIG" plant

According to Figure 18, the stator voltages of the nominal regime of DFIG and all its perturbed regimes, perfectly follow the set-point variations with good performances, also small interactions are observed during the change of set-point due to a weak coupling.

In the subsequent results, a sinusoidal signal is applied to the input of the closed-loop controlled system with:

$r(t) = V_{ref}\sin(\omega.t)$, where the pulsation is defined by $\omega = 2\pi.f$ and the frequency f is set at 50Hz, the set-point amplitude is V_{ref} varies from 100V to 220V.

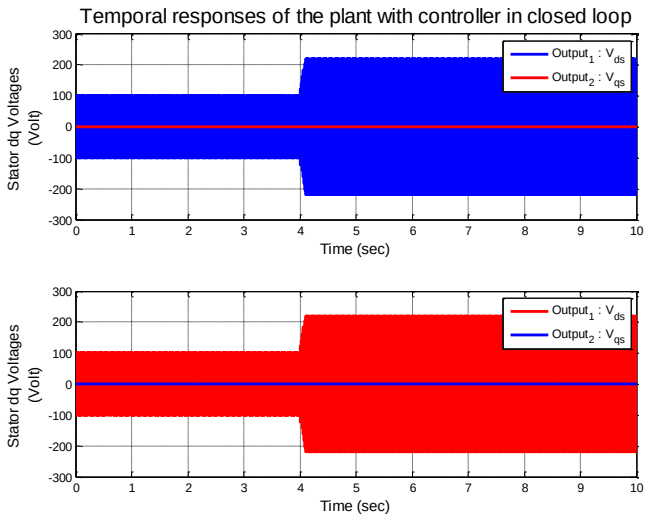

Figure 19. Temporal responses of the stator voltages with reference tracking

Figure 19, shows the output signals V_{ds} and V_{qs} during the transition from 100V to 220V.

The enlargement of the transitional phase for nominal and disturbed plants (DFIG) is given in Figures 20 and 21 respectively.

Figure 20 presents the nominal DFIG system without uncertainty while Figure 21 illustrates the different uncertain models of the DFIG, from these representations we see that the frequency is maintained at 50 Hz, and that the outputs Vds, Vqs of the nominal model (Figure 20) and uncertain (Figure 21) follow the reference variation near 100 V to 220 V with a low tracking error and an appreciable response time, we also note a low coupling.

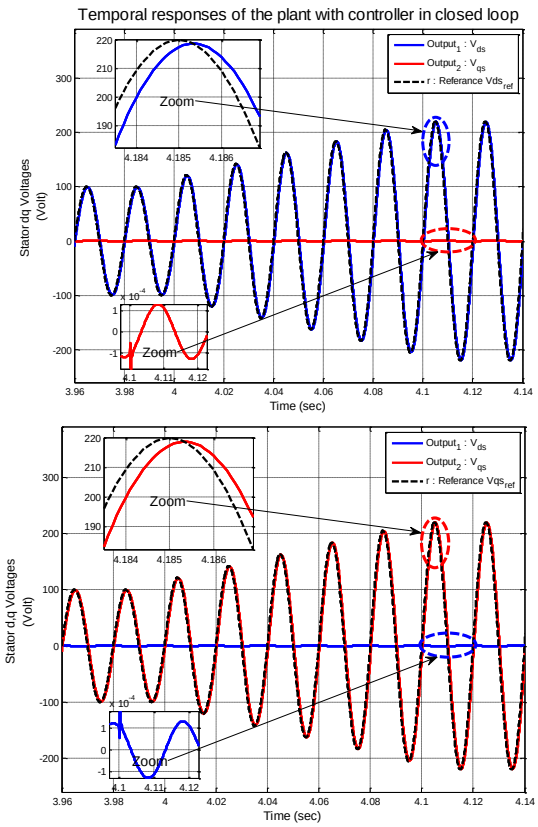

Figure 20. Enlargement of the stator output voltages of the nominal plant

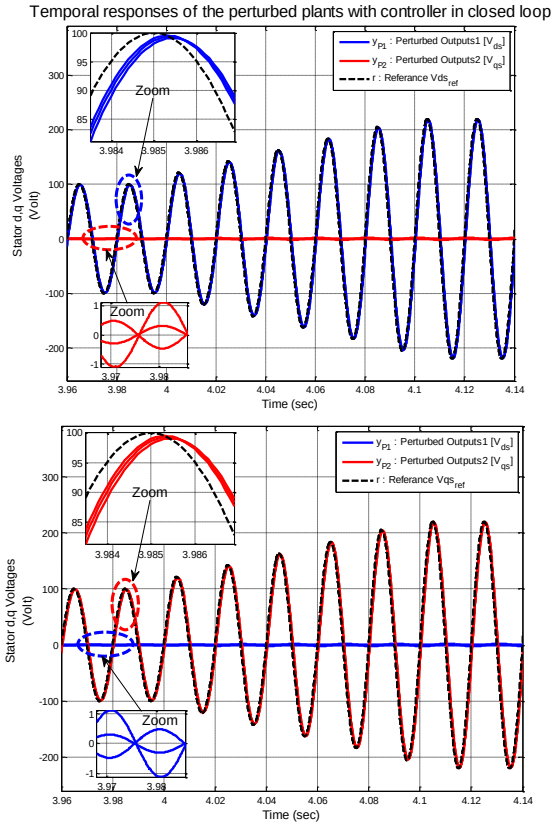

Figure 21. Enlargement of the stator output voltages of the perturbed plant

6. CONCLUSION

In this paper, we applied the LMI approach for the design of a robust LQG controller to control the doubly-fed asynchronous machine (DFIG) of a aero-generator subject to disturbance influences.

The robust command was developed using the LQG command synthesis method by the LMI approach where a Kalman estimator is presented as a LMI-EVP problem (eigenvalue problem) obtained from the Dual correspondences existing in the LQ control reformulated into LMI-EVP problem, in order to solve them by the convex optimization. Then the control and the estimator were combined into a single controller and applied to the DFIG model. The LQG regulator is adjusted in the frequency domain by the concept of loop-shaping by acting on the weighting matrices of the LQ control to guarantee the robust stability condition and then on the noise covariance matrices of the Kalman estimator to reconstruct the unmeasured state of the DFIG "rotor flux" and to ensure the robustness condition on the desired performances.

The results obtained in simulation showed the LMI approach satisfaction for the design of the robust LQG controller where its application on the DFIG model has been approved successfully the robustness guarantee of the stability and performances despite the influences of the disturbances and the parametric variations affecting DFIG.

In general, the LQG control is well-designed to be implemented in practice, especially for rotating systems as in our case study, application to the DFIG for the production of electrical energy in the face of possible parametric uncertainties. In practice, the interest of this control is to use of the Kalman estimator to reconstruct the difficult-to-measure

rotor flux state variables, and the robust state feedback control reduces the influence of uncertainties and keeps the system stable with good performance. Finally, this study is a tool that allows automation engineers to implement robust LQG controller easily.

Likewise, it is possible to apply the same design methodology using other robust controllers such as: H_∞, mixed H_2/H_∞ and μ-analysis, by the LMI approach which will be interesting to implement and to make a comparative study in the next publication.

REFERENCES

[1] Nelson, V. (2009). Wind Energy: Renewable Energy and the Environment. CRC Press. https://doi.org/10.1201/9781420075694

[2] Johnson, G.L. (1985). Wind Energy Systems. Englewood Cliffs, NJ: Prentice-Hall. pp. 147-149.

[3] Castaldi, P., Tilli, A. (2005). Parameter estimation of induction motor at standstill with magnetic flux monitoring. IEEE Transactions on Control Systems Technology, 13(3): 386-400. http://dx.doi.org/10.1109/tcst.2004.841643

[4] Engelhardt, S., Erlich, I., Feltes, C., Kretschmann, J., Shewarega, F. (2010). Reactive power capability of wind turbines based on doubly fed induction generators. IEEE Transactions on Energy Conversion, 26(1): 364-372. http://dx.doi.org/10.1109/tec.2010.2081365

[5] Athans, M. (1971). The role and use of the linear-quadratic-Gaussian-stochastic problem in control system design. IEEE Transactions on Automatic Control, 16(6): 529-552. http://dx.doi.org/10.1109/tac.1971.1099818

[6] Davis, M.H.A. (1977). Linear Estimation and Stochastic Control. Chapman and Hall, London.

[7] Wonham, W.M. (1968). On the separation theorem of stochastic control. SIAM Journal on Control, 6(2): 312-326. https://doi.org/10.1137/0306023

[8] Anderson, B.D.O., Moore, J.B. (1971). Linear Optimal Control. Prentice-Hall, INC. Englewood Cliffs, N.J.

[9] Poitiers, F., Bouaouiche, T., Machmoum, M. (2009). Advanced control of a doubly-fed induction generator for wind energy conversion. Electric Power Systems Research, 79(7): 1085-1096. https://doi.org/10.1016/j.epsr.2009.01.007

[10] Kalman, R.E. (1964). When is a linear control system optimal? Journal of Basic Engineering, Series D, 86(1): 51-60. https://doi.org/10.1115/1.3653115

[11] Safonov, M., Athans, M. (1977). Gain and phase margin for multiloop LQG regulators. IEEE Transactions on Automatic Control, 22(2): 173-179. http://dx.doi.org/10.1109/tac.1977.1101470

[12] Doyle, J., Stein, G. (1981). Multivariable feedback design: Concepts for a classical/modern synthesis. IEEE transactions on Automatic Control, 26(1): 4-16. http://dx.doi.org/10.1109/tac.1981.1102555

[13] Athans, M. (1986). A tutorial on the LQG/LTR method. In 1986 American Control Conference, pp. 1289-1296. https://doi.org/10.23919/ACC.1986.4789131

[14] Stein, G., Athans, M. (1987). The LQG/LTR procedure for multivariable feedback control design. IEEE Transactions on Automatic Control, 32(2): 105-114. http://dx.doi.org/10.1109/tac.1987.1104550

[15] Galimidi, A.R., Barmish, B.R. (1985). The constrained Lyapunov problem and its application to robust output feedback stabilization. In 1985 American Control Conference, pp. 433-439. https://doi.org/10.23919/ACC.1985.4788652

[16] Feron, E., Balakrishnan, V., Boyd, S., El Ghaoui, L. (1992). Numerical methods for H_2 related problems. In 1992 American Control Conference, Chicago, USA, pp. 2921-2922. https://doi.org/10.23919/ACC.1992.4792678

[17] Boyd, S., El Ghaoui, L., Feron, E., Balakrishnan, V. (1994). Linear matrix inequalities in system and control theory. SIAM Studies in Applied Mathematics. https://doi.org/10.1137/1.9781611970777

[18] Nesterov, Y., Nemirovskii, A. (1994). Interior-Point Polynomial Algorithms in Convex Programming. Society for Industrial and Applied Mathematics.

[19] Chadli, M., Borne, P. (2012). Multiple Models Approach in Automation: Takagi-Sugeno Fuzzy Systems. John Wiley & Sons.

[20] Soens, J., Driesen, J., Belmans, R. (2005). Equivalent transfer function for a variable speed wind turbine in power system dynamic simulations. International Journal of Distributed Energy Resources, 1(2): 111-133. https://doi.org/10.1007/s40565-018-0410-8

[21] Soens, J., Driesen, J., Belmans, R. (2004). Wind turbine modeling approaches for dynamic power system simulations. IEEE Young Researchers Symposium in Electrical Power Engineering--Intelligent Energy Conversion, (CD-Rom), Delft, The Netherlands.

[22] Soens, J., Van Thong, V., Driesen, J., Belmans, R. (2003). Modeling wind turbine generators for power system simulations. In European Wind Energy Conference EWEC, Madrid, pp. 16-19.

[23] Lerch, E., Ruhle, O. (2005). Dynamic simulation of DFIGs for wind power plants. In 2005 International Power Engineering Conference, pp. 1-98. http://dx.doi.org/10.1109/IPEC.2005.206886

[24] Ekanayake, J.B., Holdsworth, L., Wu, X.G., Jenkins, N. (2003). Dynamic modeling of doubly-fed induction machine wind-generators. IEEE Transactions on Power Systems, 18(2): 803-809. https://doi.org/10.1109/TPWRS.2003.811178

[25] Mekki, M., Boulouiha, H.M., Allali, A., Denai, M. (2021). Impact of the integration of a STATCOM controlled by LQG/H2 regulator in an energy system. European Journal of Electrical Engineering, 23(5): 361-370. https://doi.org/10.18280/ejee.230502

[26] Fan, L., Miao, Z. (2015). Modeling and Analysis of Doubly Fed Induction Generator Wind Energy Systems. Academic Press. https://doi.org/10.1016/C2014-0-03793-8

[27] Meera, G.S., Divya, N.A. (2015). Dynamic modeling and analysis of DFIG based wind turbine for variable wind speed. IJSTE - International Journal of Science Technology & Engineering, 2(2): 210-217.

[28] Bouras, L., Zennir, Y., Bourourou, F. (2013). Direct torque control with SVM based a fractional controller: Applied to the induction machine. 3rd IEEE International Conference on Systems and Control (ICSC 2013), Algiers, Algeria, pp. 702-707. http://dx.doi.org/10.1109/ICoSC.2013.6750936

[29] Ju, Y., Ge, F., Wu, W., Lin, Y., Wang, J. (2016). Three-phase steady-state model of doubly fed induction generator considering various rotor speeds. IEEE Access,

4: 9479-9488. http://dx.doi.org/10.1109/access.2016.2646683
[30] Milich, D., Valavani, L., Athans, M. (1986). Feedback system design with an uncertain plant. In 1986 25th IEEE Conference on Decision and Control, pp. 441-446. http://dx.doi.org/10.1109/cdc.1986.267296
[31] Skogestad, S., Postlethwaite, I. (2005). Multivariable Feedback Control: Analysis and Design. John Wiley & Sons.
[32] Khalil, I.S., Doyle, J.C., Glover, K. (1996). Robust and Optimal Control. Prentice Hall.
[33] Ostertag, E. (2011). Mono-And Multivariable Control and Estimation: Linear, Quadratic and LMI Methods. Springer Science & Business Media.
[34] Dragan, V., Morozan, T., Stoica, A.M. (2006). Mathematical Methods in Robust Control of Linear Stochastic Systems. New York: Springer. https://doi.org/10.1007/978-1-4614-8663-3
[35] Rezaei, H., Mohamed, S., Esfanjani, R.M., Nahavandi, S. (2014). Improved robust Kalman filtering for uncertain systems with missing measurements. In: Loo, C.K., Yap, K.S., Wong, K.W., Beng Jin, A.T., Huang, K. (eds) Neural Information Processing. ICONIP 2014. Lecture Notes in Computer Science, vol 8836. Springer, Cham. https://doi.org/10.1007/978-3-319-12643-2_62
[36] Kalman, R.E. (1960). A new approach to linear filtering and prediction problems. Transactions of ASME, Journal of Basic Engineering, Series D, 82(1): 35-45. https://doi.org/10.1115/1.3662552
[37] Scherer, C., Gahinet, P., Chilali, M. (1997). Multiobjective output-feedback control via LMI optimization. IEEE Transactions on Automatic Control, 42(7): 896-911. https://doi.org/10.1109/9.599969
[38] Slotine, J.J.E., Li, W. (1991). Applied Nonlinear Control. Englewood Cliffs, NJ: Prentice Hall.
[39] Dullerud, G.E., Paganini, F. (2013). A Course in Robust Control Theory: A Convex Approach. Springer Science & Business Media. https://doi.org/10.1007/978-1-4757-3290-0